Soil Temperature and Soil Moisture Patterns in a Himalayan Alpine Treeline Ecotone

Authors: Müller, Michael, Schwab, Niels, Schickhoff, Udo, Böhner, Jürgen, and Scholten, Thomas

Source: Arctic, Antarctic, and Alpine Research, 48(3) : 501-521

Published By: Institute of Arctic and Alpine Research (INSTAAR), University of Colorado

URL: https://doi.org/10.1657/AAAR0016-004

Arctic, Antarctic, and Alpine Research, Vol. 48, No. 3, 2016, pp. 501–521
DOI: http://dx.doi.org/10.1657/AAAR0016-004

Soil temperature and soil moisture patterns in a Himalayan alpine treeline ecotone

Michael Müller[1,*], Niels Schwab[2], Udo Schickhoff[2], Jürgen Böhner[2], and Thomas Scholten[1]

[1]Department of Geosciences, Chair of Soil Science and Geomorphology, University of Tübingen, Rümelinstraße 19-23, 72070 Tübingen, Germany
[2]CEN Center for Earth System Research and Sustainability, Institute of Geography, University of Hamburg, Bundesstraße 55, 20146 Hamburg, Germany
[*]Corresponding author's email: michael.mueller@uni-tuebingen.de

A B S T R A C T

Soil properties in alpine treeline ecotones are insufficiently explored. In particular, an extensive monitoring of soil moisture conditions over a longer period of time is rare, and the effects of soil moisture variability on alpine treelines have not received adequate attention yet. Soil temperature patterns are generally well documented, and soil temperature is considered a key factor in limiting tree growth at both global and local scales. We performed a 2½-year monitoring in a near-natural treeline ecotone in Rolwaling Himal, Nepal. In this paper, we present new findings on spatiotemporal soil temperature and moisture variability in relation to topographical features and vegetation patterns (variations in stand structures and tree physiognomy). Our results show a growing season mean soil temperature of 7.5 ± 0.6 °C at 10 cm depth at the Rolwaling treeline. Multivariate statistical analyses yield a significant relation between soil temperatures and the variability in tree height, crown length, crown width, and leaf area index (LAI). In turn, soil temperature variability is controlled by the tree physiognomy itself. Soil moisture conditions (available water capacity, 0–10 cm) appear to be less substantial for current stand structures and tree physiognomy. In turn, tree physiognomy patterns control soil moisture, which additionally is affected by snow cover. In Rolwaling, shallow and coarse-grained soils cause low water-holding capacities, and thus a remarkable amount of water percolates from topsoils to subsoils. In the alpine tundra with missing forest canopy, year-round lowest available water capacities are additionally caused by high solar radiation, wind, and thus high evaporation. We assume low soil moisture availability causing largely prevented tree regeneration especially in the alpine tundra.

We conclude that soil temperature and moisture patterns reflect tree physiognomy patterns. The latter cause disparities in soil temperature and moisture conditions inside and outside of the closed forest by shading effects and differences in leaf fall.

Introduction

Tree growth at high altitudes is assumed to be limited by heat deficiency (low air and soil temperatures, e.g., Körner, 1998a, 1998b, 2012; Körner and Paulsen, 2004; Wieser and Tausz, 2007; Holtmeier, 2009). A considerable amount of soil temperature (ST) data is available from alpine treelines around the globe (Müller et al., 2016). At a global scale, a growing season mean ST of 6.4 ± 0.7 °C has been suggested as a threshold temperature under trees at treeline elevations (Körner, 2012). At

a local scale, a wide range of 5 to 12 °C occurs worldwide for growing season mean ST at alpine treelines (Müller et al., 2016). Many researchers had discussed whether tree growth in alpine treeline ecotones is limited solely by low temperatures (e.g., by an impact on meristematic processes or on photosynthesis; Hoch and Körner, 2005, 2009), or whether it is limited or modified by different abiotic and biotic factors (e.g., Holtmeier, 2009; Körner, 1998a, 2012). A detailed overview of the state of knowledge with regard to the effects of soil properties on tree growth is given in Müller et al. (2016). In contrast to ST data from the immediate vicinity of alpine treeline elevations, spatiotemporal ST data for entire treeline ecotones including subalpine forest and alpine tundra are rare and mostly cover short monitoring periods of <1 year only (e.g., Walter and Medina, 1969; Liu and Luo, 2011; McNown and Sullivan, 2013; Paulsen and Körner, 2014).

To date, only a few studies have investigated soil moisture (SM) and its effect on tree growth at high altitudes in more detail (Leuschner and Schulte, 1991; Gieger and Leuschner, 2004; Köhler et al., 2006; Liu and Luo, 2011; Öberg and Kullman, 2012; McNown and Sullivan, 2013; Paulsen and Körner, 2014; Peters et al., 2014). Thus, spatiotemporal distribution patterns of SM conditions in alpine treeline ecotones are insufficiently documented in literature (Müller et al., 2016). In general, modeling of plant-water relations is impeded due to an overall heterogeneous mountain terrain, and the hardly determinable rooting depths of plants (Paulsen and Körner, 2014). At a local scale, alpine treelines vary in SM available for plant growth, which in turn highly depends on the winter snow cover, and its removal and redeposition by wind (Hessl and Baker, 1997; Hättenschwiler and Smith, 1999; Malanson et al., 2011; Paulsen and Körner, 2014). Some case studies in different treeline environments have shown tree growth at treelines to be constrained by low SM availability rather than by low ST (Leuschner and Schulte, 1991; Liang et al., 2014; González de Andrés et al., 2015). It has been suggested that growth conditions for trees and young growth are impeded by water shortage prior to the growing season caused by an insufficient snow cover in winter, and by still frozen soils in spring, respectively (Balducci et al., 2013). During summer, increasing SM stress may also result from a warming-induced earlier onset of snowmelt (Öberg and Kullman, 2012). Further, SM stress has been demonstrated to constrain seedling establishment (e.g., Weisberg and Baker, 1995; Hessl and Baker, 1997; Lloyd and Graumlich, 1997; Camarero and Gutiérrez, 2004; Daniels and Veblen, 2004; Holtmeier and Broll, 2010; Moyes et al., 2015) and tree growth in different alpine treeline ecotones (e.g., Jacoby and D'Arrigo, 1995; Lloyd and Graumlich, 1997; Öberg and Kullman, 2012). A literature review by Müller et al. (2016) concluded that tree growth at semiarid to arid subtropical, and oceanic island treelines is predominantly affected by seasonal drought stress (e.g., Leuschner and Schulte, 1991; Biondi, 2001; Daniels and Veblen, 2004; Gieger and Leuschner, 2004; Morales et al., 2004; Lara et al., 2005). However, the latter outcome would gain in importance if there were a larger amount of studies not only from those regions, but from a greater variety of treeline environments (Müller et al., 2016). In contrast, some studies do not attribute SM a major role in controlling tree growth, at least at a global scale (e.g., Hoch and Körner, 2005). This holds true for a treeline ecotone in the Sergyemla Mountains, Tibet, where Liu and Luo (2011) could not find a significant relationship between SM variability, and vegetation and topographical patterns. With regard to the Himalaya, information on ST and SM patterns and their interactions with vegetation patterns is scarce. Therefore, the aims of this study were

1. to monitor and analyze spatiotemporal ST and SM data from a near-natural treeline ecotone in Rolwaling Himal, Nepal, over a longer period of time, and
2. to determine the interactions between ST and SM, topography, and variations in stand structures and tree physiognomy at a local scale.

Materials and Methods

Study Area

The study area is located in the northeast part of Central Nepal (27°54′N, 86°22′E; Fig. 1). The experimental area is situated on the unsettled north-exposed slope opposite to the village of Beding in Rolwaling Himal.

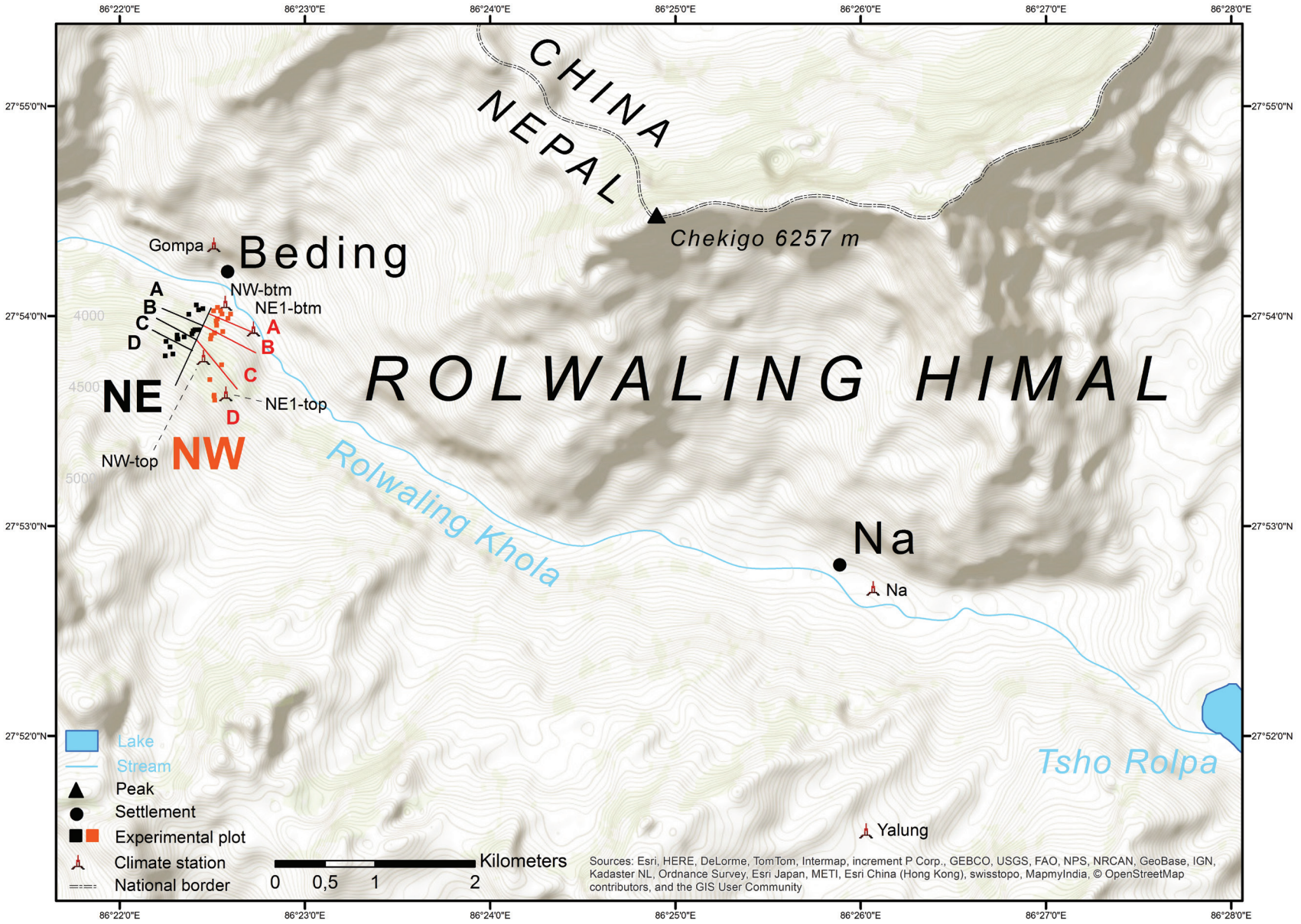

FIGURE 1. Study area and monitoring sites for soil temperature and soil moisture in Rolwaling Himal, Nepal. Experimental design includes two investigated altitudinal transects (NE = northeast exposition [black], NW = northwest exposition [red]) including four altitudinal zones (A, B, C, D), and location of experimental plots and climate stations (btm = bottom, top, Gompa, Na, Yalung). The map is adopted and modified from Müller et al. (2016).

Upper subalpine forests are primarily composed of *Betula utilis* and *Abies spectabilis*, with *Rhododendron campanulatum*, *Sorbus microphylla, Acer caudatum,* and *Prunus rufa* forming a second tree layer (Schwab et al., 2016). Closed forests merge into a broad krummholz belt of *Rhododendron campanulatum* at ~3900 m a.s.l. (NW exposition, cf. Figs. 1 and 2) and ~4000 m a.s.l. (NE exposition), respectively, which gives way to alpine tundra (*Rhododendron* dwarf shrub heaths) at ~4000 and ~4100 m a.s.l., respectively. Dwarf shrubs are interspersed by a small number of low-growing individuals (diameter in breast height [dbh] < 7 cm) or young growth of *Abies spectabilis*, *Betula utilis*, and in a higher amount of *Rhododendron campanulatum*. Occasionally, *Sorbus microphylla* individuals with dbh ≥ 7 cm occur (Schwab et al., 2016). Total plant species richness decreases from the closed forests in the subalpine zone across the treeline ecotone and increases again in the uppermost dwarf scrub heath at the transition to alpine grassland. Due to isolation and a very low population density of the Rolwaling valley, and virtually pristine vegetation, the treeline ecotone is considered as near-natural (Schwab et al., 2016).

Soils in the study area were classified as Podzols (according to IUSS, 2006), characterized by a substantial outwash of soil organic matter and sesquioxides from topsoil to subsoil (podsolization). Podzols showed the typical sequence of Oi-Oe-Ah-Ae-Bh-Bs horizons. Litter cover strongly decreases from closed forest and krummholz to the alpine tundra.

Experimental Design and Data Collection

We used a stratified random sampling design with two transects (NE = northeast exposition, NW = northwest exposition, Figs. 1 and 2) across the treeline ecotone divided into four altitudinal zones: A (closed forest), B (uppermost closed forest), C (krummholz), and D (dwarf scrub heath/

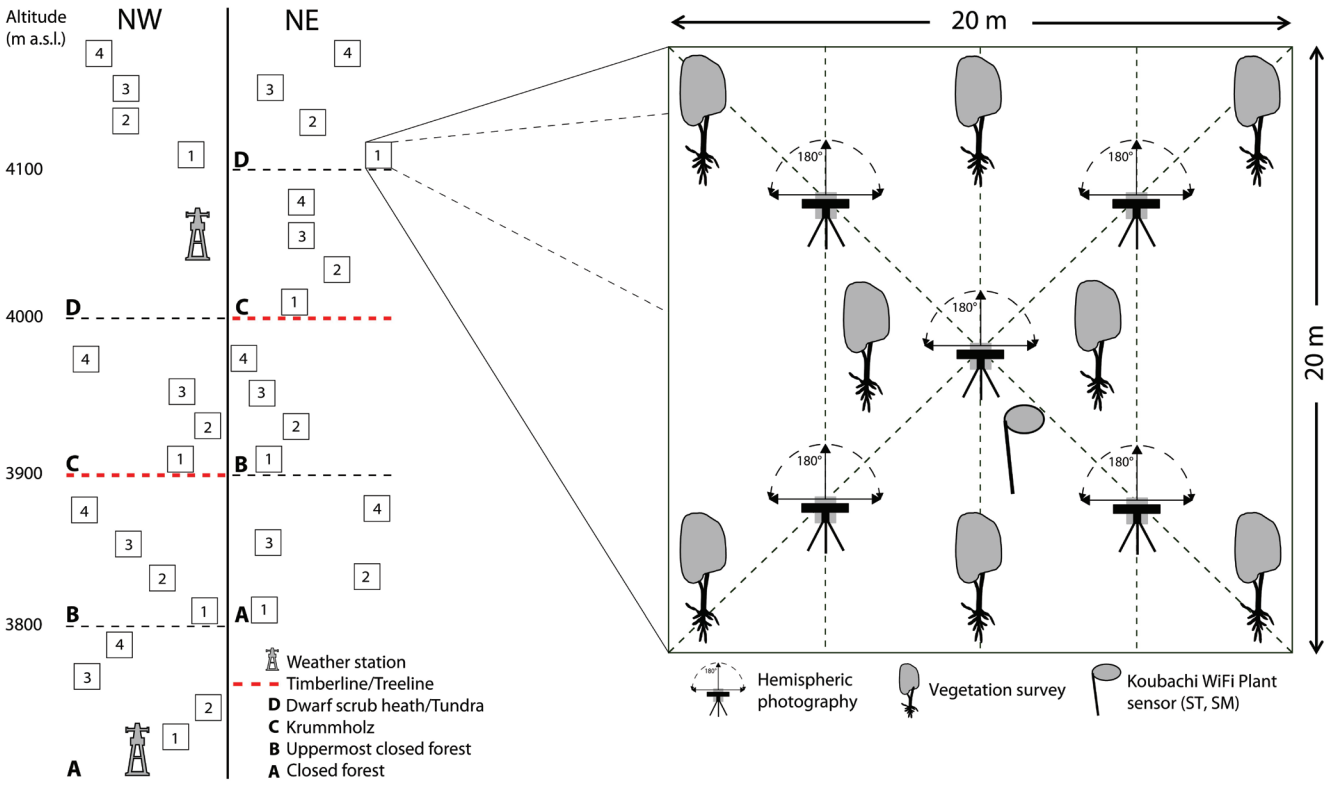

FIGURE 2. Experimental design. Schematic illustration of the two different altitudinal transects (NE = northeast exposition, NW = northwest exposition) including four experimental plots (20 m × 20 m), respectively, in each altitudinal zone (A, B, C, D). Plot design (right) is equivalent on each plot. Koubachi Wi-Fi plant sensors are available on both transects.

alpine tundra, Figs. 1 and 2). Within each zone of each altitudinal transect, four different plots (20 m × 20 m, projected on a horizontal plain) were randomly selected (Figs. 1 and 2).

On 32 plots (2 transects × 4 altitudinal zones × 4 plots, Fig. 2) Koubachi Wi-Fi plant sensors (Koubachi AG) monitored ST (°C) and SM (pF) every hour at 10 cm depth from April 2013 to October 2015, respectively. Additionally, two sensors were placed underneath the uppermost individuals *Abies spectabilis* (~5–10 m high) and *Betula utilis* (~5 m) on NE transect (equivalent to the transition from zone B to C). The sensors were modified for outdoor usage to log ST from −10 to +55 °C, and pF (decadic logarithm of the absolute value of soil water tension, nondimensional) from 0 to 5.75. We use lithium batteries, which ensure energy supply under harsh climatic conditions. Data were obtained via Wi-Fi interface. For calculation of growing season mean ST, we used the well-accepted definition of growing season by Körner and Paulsen (2004), when daily mean ST at 10 cm depth first exceed 3.2 °C until they drop again below 3.2 °C.

SM was determined as soil water content (Vol.-% or L m^{-2} dm^{-1}) from pF based on linear regression equations derived from default charts in Ad-hoc-Arbeitsgruppe Boden (2005) (cf. Table 3 later). Available water capacity (AWC, Vol.-% or L m^{-2} dm^{-1}) was calculated from SM, soil texture, and bulk density (cf. Table 3 later) according to Ad-hoc-Arbeitsgruppe Boden (2005). Soil texture was analyzed according to Blume et al. (2011), using a Sedigraph III Plus Particle Size Analyzer (Micromeritics) in the laboratory. Bulk density was determined gravimetrically after drying of the soil at 105 °C after field sampling with 100 cm^3 core cutters.

Vegetation surveys took place in April, May, July, and August 2013, and in September 2014. We measured diameter at breast height (130 cm, dbh), and tree height of all trees with dbh ≥ 7 cm (cf. Schwab et al., 2016). Crown length (length of crown from trunk to terminal bud), and crown width were determined according to van Laar and Akça (2007). The number of tree individuals (dbh ≥ 7 cm) was counted on each experimental plot. Leaf area index (LAI) was measured using hemispheric photography. The camera (Nikon Coolpix 8400) includes a wide-angle fisheye lens (Nikon Fisheye Converter FC-E9), which was aligned to the free sky obtaining an angle of view of 180°. Five photos per plot (cf. Fig. 2) were taken in a cross pattern at 90 cm above ground at consistent clouded sky to enable an optimal documentation of light conditions (diffuse radiation component). Photos were taken from 22 to 27 September 2014 on NW transect, and from 09 to 21 September 2014 on NE transect. Using HemiView software (HEMIv9), all photos were analyzed for LAI, and mean LAI per plot computed.

Statistical Analyses

Statistical analyses were conducted using the free programming language R, version 3.1.2 (R Development Core Team, 2014) by applying R-packages *car* (Fox and Weisberg, 2011), *PMCMR* (Pohlert, 2014), *stats* (R Development Core Team, 2014), *shape* (Soetaert, 2014), *vegan* (Oksanen et al., 2015), and *zoo* (Zeileis and Grothendieck, 2005).

Data gaps of ST and soil pF were small (<15 days) and were interpolated and extrapolated using R-packages *zoo* and *stats*. Data were transferred to ArcMap 10.1, and georeferenced based on GPS data from field measurements during soil sampling. In ArcMap, we used IDW (inverse distance weighting) as deterministic method for spatial interpolation.

We performed multivariate statistical analyses to test the relation between the independent soil variables temperature (ST) and available water capacity (AWC), and the dependent vegetation variables dbh, LAI, tree height, crown width, crown length, and number of tree individuals. Due to multicollinearity, soil moisture (SM) was excluded from analyses. The large data sets of ST and AWC contained the means from each experimental plot (NE-A1 to NE-D4, NW-A1 to NW-D4) for the entire measurement period (01 May 2013 to 31 October 2015), and for the different seasons (MAM 14, 15, JJAS 13, 14, 15, ON 13, 14, DJF 13/14, 14/15, cf. Results). For the dependent variables, we also used means from each experimental plot. In a first step prior to a redundancy analysis (RDA), we applied a principal component analysis (PCA) for each of the two data sets ST and AWC individually. The reasons for that were

to avoid multicollinearity among the many variables that represent ST and AWC, respectively, and to create the best fitting model of principal components for each of the two variables before we performed an RDA. Using the principal components in an RDA, we tested the effects of ST and AWC on vegetation variables with regard to the diverse altitudinal zones (A, B, C, D), and to different aspects (NW, NE). The results were verified by applying a multivariate multiple regression analysis (MMR), and subsequent MANOVA/ANOVA.

We further tested the influence of diverse environmental variables on ST, AWC, and SM by applying multivariate linear regression analyses. Therefore, we used a larger data set consisting of the before-mentioned vegetation variables complemented by soil related variables (texture, bulk density, thickness of litter layer), and topographical variables (aspect [northness = cos(exposition)], elevation in m a.s.l). To avoid multicollinearity between independent variables, we tested them using the *vif.cca* function in R. To create the best-fitting model (MMR) for the explanation of all dependent variables, and of each dependent variable individually, we conducted backward selection using the *ordistep* function from the *vegan* package in R.

Results

Soil Temperature

Mean ST (period: 1 May 2013–31 October 2015) at 10 cm depth showed a significant decrease with elevation (m a.s.l.) on NW transect (Spearman $r = -0.71$, $p < 0.01$). In contrast, no significant decrease was detected on NE transect ($r = -0.04$, $p = 0.88$). Also during growing season (cf. Fig. 3), NW showed a significant decline of mean ST with elevation (m a.s.l.) (2013: $r = -0.74$, $p < 0.001$, 2014: $r = -0.82$, $p < 0.01$, 2015: $r = -0.81$, $p < 0.001$) which was not found on NE (2013: $r = 0.15$, $p = 0.55$, 2014: $r = -0.01$, $p = 0.99$, 2015: $r = 0.28$, $p = 0.25$). Despite altitudinal zones A–D being located 100 m lower in elevation on NW (cf. Figs. 1 and 2), mean STs during growing season of NW A–D were slightly lower (2013: 7.7 ± 0.8 °C, 2014: 7.4 ± 0.8 °C, 2015: 7.4 ± 0.7 °C) compared to NE (2013: 7.8 ± 0.6 °C, 2014: 7.7 ± 0.6 °C, 2015: 7.5 ± 0.6 °C). At treeline (transition from uppermost closed forest [B] to krummholz [C]), we calculated a growing season mean ST of 7.5 ± 0.6 °C as mean of both transects for the growing seasons in 2013, 2014, and 2015 (cf. Fig. 3). Hereby, mean STs at treeline were slightly higher or same on NW as compared to NE (Fig. 3).

We found altitudinal zone-specific spatial patterns in ST. On NW, mean ST (period: 1 May 2013–31 October 2015) showed a strong decline from AB (4.56 °C, 4.76 °C) to CD (3.29 °C, 2.95 °C). On NE, a temperature gradient occurred from AB (4.05 °C, 4.68 °C) to C (3.28 °C); however, a higher temperature was measured in D (4.17 °C). A variance analysis (Kruskal Wallis) with subsequent post-hoc Nemenyi (Tukey) test revealed major differences ($p < 0.0001$) in daily mean ST between altitudinal zones on both transects. On NW, zones A and B ($p = 0.28$), and C and D ($p = 0.12$) showed similar variances. On NE, zones A and D ($p = 0.66$) and B and D ($p = 0.30$) did not differ significantly from each other.

With regard to different seasons, mean ST in spring (MAM) was commonly higher on NE (Table 1, Fig. 4). Conversely, we found an opposite spatial trend for autumn (ON) and winter (DJF), except for the alpine tundra (zone D). In summer (JJAS), temperature was similar on both transects, except for the alpine tundra where NE was marked by on average 2 K higher temperatures than NW (Table 1, Fig. 4).

Overall, we measured year-round higher STs in D compared to C, and slightly higher or similar STs compared to A on NE. This was not found for NW, where lowest STs occurred in D, especially in summer (JJAS). Higher STs in D compared to C were found in ON 13 and DJF 13/14 only, and similar STs were measured in MAM 14 (Table 1). Winter (DJF) STs on both transects were similar or even colder in A compared to C and D, and were warmest in B (Table 1, cf. Fig. 4). Also in autumn (ON) and spring (MAM), higher STs were measured in B compared to A. In general, STs in winter 2014/2015 (DJF 14/15) were markedly higher than in winter 2013/2014 (DJF 13/14) (Table 1). Likewise, STs in spring 2015 (MAM 15) exceeded those of spring 2014 (MAM 14) (Table 1).

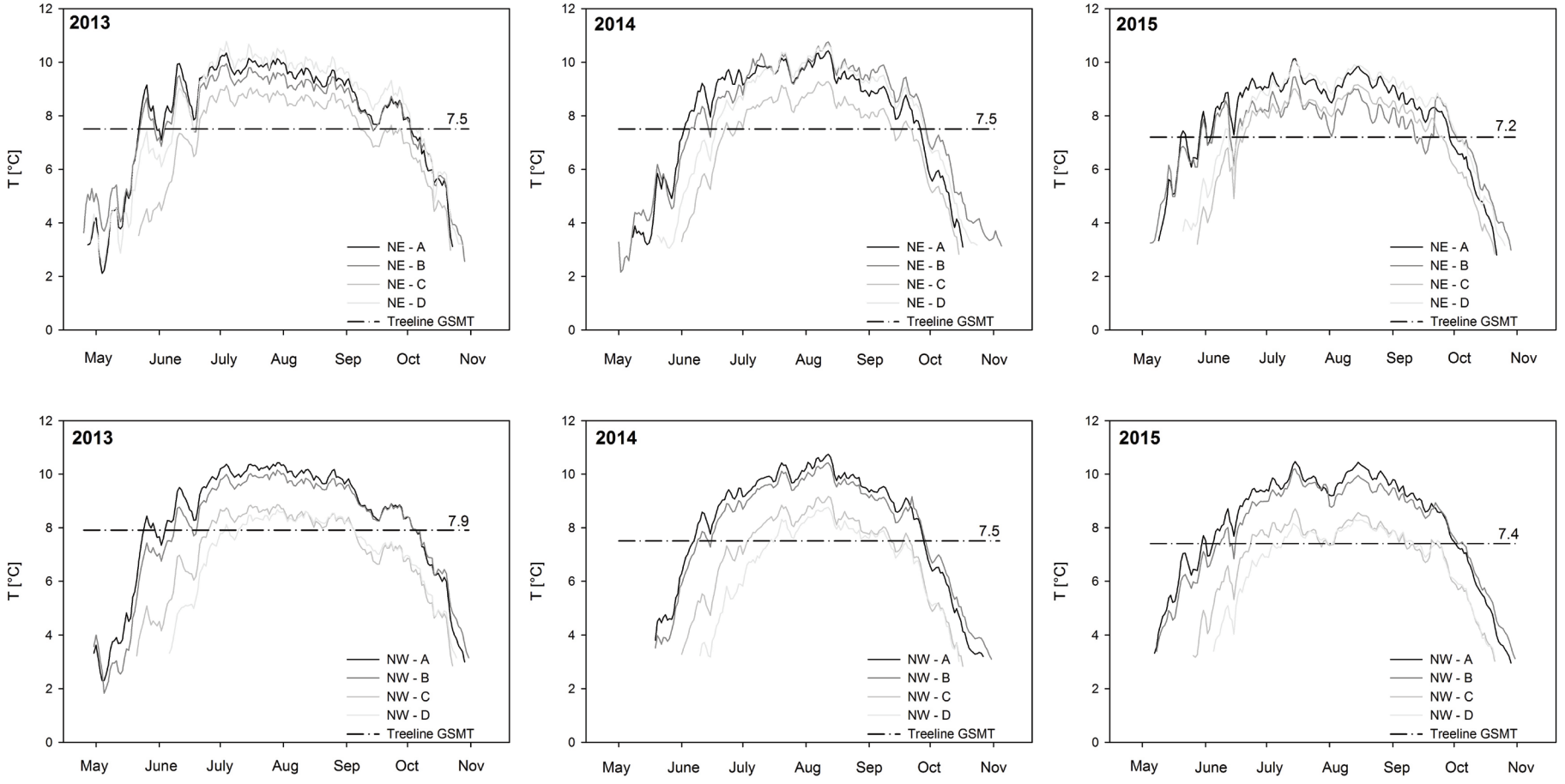

FIGURE 3. Daily mean soil temperatures during growing season in 2013, 2014, and 2015 at 10 cm depth in altitudinal zones A (closed forest), B (uppermost closed forest), C (krummholz), and D (alpine tundra) on NE (top) and NW transect (bottom). Treeline GSMT = growing season mean temperature at 10 cm soil depth at treeline.

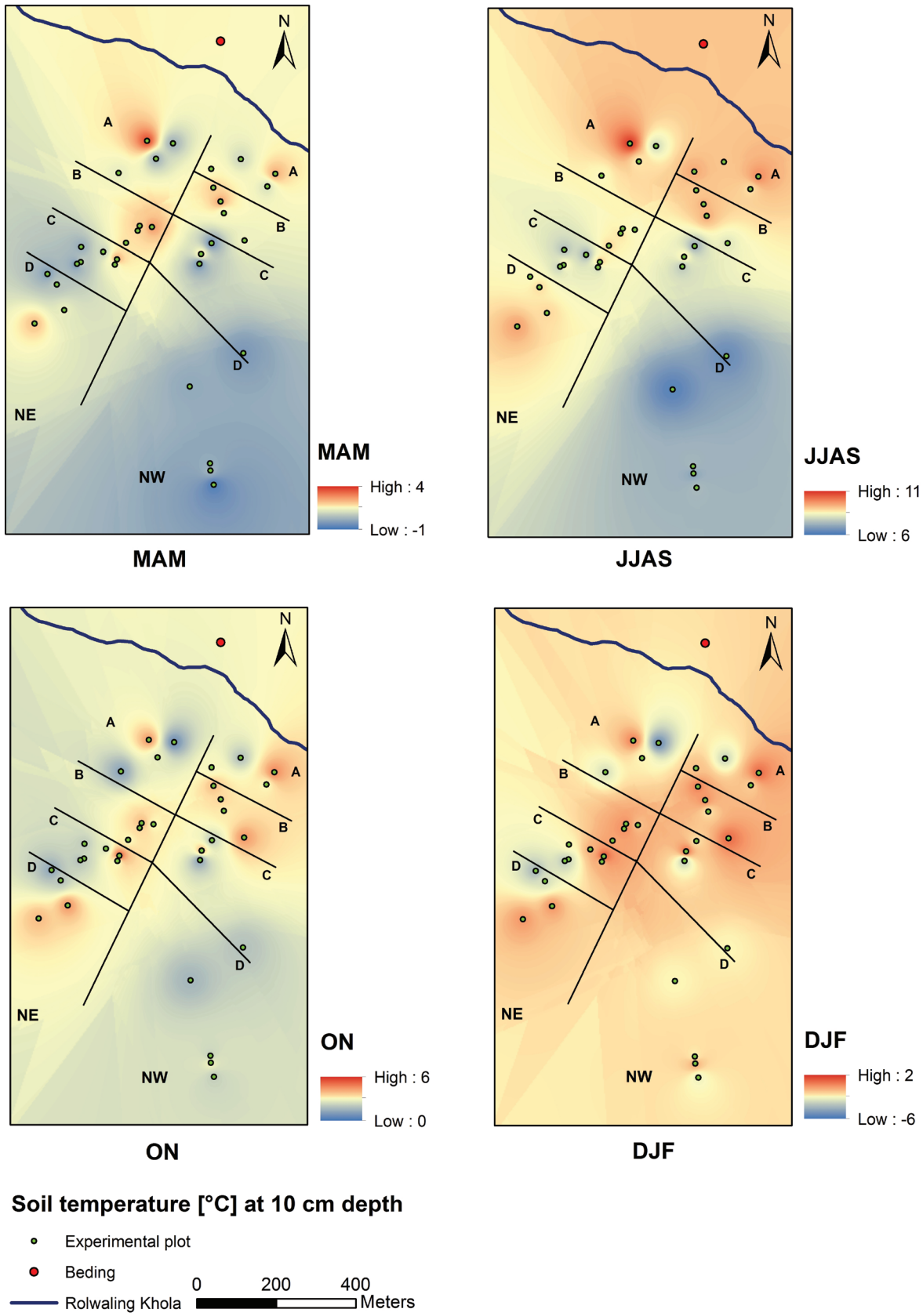

FIGURE 4. Spatiotemporal distribution of soil temperatures at 10 cm depth. A, B, C, D = altitudinal zones. NW = northwest. NE = northeast. MAM = spring (March, April, May), JJAS = summer (June, July, August, September), ON = autumn (October, November), DJF = winter (December, January, February).

TABLE 1

Mean seasonal soil temperatures (± s.e.) at 10 cm depth in the altitudinal zones A, B, C, and D on the NE and NW transect. Different letters indicate significant differences at $p < 0.05$ by Post-hoc Nemenyi (Tukey) test.

Transect	Season	A	B	C	D
NE	AM 13 [1]	4.4 ± 1.2 [a]	5.1 ± 0.7 [b]	2.5 ± 1.2 [c]	4.7 ± 0.7 [d]
	JJAS 13	9.2 ± 1.2 [a]	8.9 ± 0.5 [b]	7.9 ± 0.7 [c]	9.4 ± 0.7 [a]
	ON 13	2.5 ± 1.6 [a]	3.3 ± 1.0 [ab]	2.3 ± 0.4 [bc]	2.9 ± 1.6 [c]
	DJF 13/14	–2.9 ± 2.0 [a]	–0.6 ± 0.7 [b]	–3.2 ± 1.5 [a]	–2.6 ± 2.0 [c]
	MAM 14	1.2 ± 1.5 [ab]	1.9 ± 0.8 [b]	0.2 ± 0.8 [a]	1.0 ± 1.0 [b]
	JJAS 14	9.1 ± 1.2 [a]	9.2 ± 1.2 [a]	7.6 ± 0.8 [b]	8.9 ± 0.6 [a]
	ON 14	2.0 ± 1.6 [a]	3.5 ± 0.8 [b]	1.9 ± 0.4 [b]	2.8 ± 1.5 [c]
	DJF 14/15	–1.7 ± 2.5 [a]	0.0 ± 0.4 [b]	–1.1 ± 1.2 [c]	–0.8 ± 1.9 [c]
	MAM 15	1.5 ± 1.9 [ac]	2.3 ± 0.8 [bd]	0.5 ± 0.7 [acd]	0.9 ± 1.1 [bcd]
	JJAS 15	8.8 ± 1.5 [a]	8.0 ± 0.6 [b]	7.8 ± 0.7 [b]	8.7 ± 0.4 [a]
NW	AM 13 [1]	4.2 ± 1.0 [a]	3.7 ± 1.2 [b]	2.8 ± 1.1 [c]	1.3 ± 0.7 [d]
	JJAS 13	9.5 ± 0.6 [a]	9.2 ± 0.7 [b]	7.7 ± 1.0 [c]	7.3 ± 0.9 [c]
	ON 13	3.2 ± 1.1 [ab]	3.9 ± 0.3 [bc]	2.4 ± 1.2 [c]	2.7 ± 0.6 [c]
	DJF 13/14	–1.9± 1.8 [a]	–0.8 ± 0.9 [b]	–2.4 ± 1.8 [a]	–2.1 ± 1.1 [a]
	MAM 14	0.8 ± 1.0 [a]	1.3 ± 0.8 [b]	0.0 ± 1.1 [a]	0.0 ± 0.6 [a]
	JJAS 14	9.3 ± 0.6 [a]	9.0 ± 0.8 [a]	7.4 ± 1.1 [b]	6.7 ± 0.6 [c]
	ON 14	3.0 ± 1.3 [a]	3.7 ± 1.0 [b]	2.0 ± 1.2 [b]	1.6 ± 0.6 [b]
	DJF 14/15	–0.2 ± 1.5 [a]	0.6 ± 1.2 [b]	–0.6 ± 1.6 [a]	–1.1 ± 0.7 [c]
	MAM 15	2.1 ± 0.9 [a]	2.2 ± 0.8 [a]	0.4 ± 1.1 [b]	–0.2 ± 0.7 [b]
	JJAS 15	9.3 ± 0.5 [a]	8.9 ± 0.5 [a]	7.4 ± 1.0 [b]	7.0 ± 0.4 [b]

[1] Data in April are available from 18.04.2013 (dd.mm.yyyy).

Notes: AM 13 = April–May 2013, MAM = spring (March, April, May). JJAS = summer (June, July, August, September), ON = autumn (October, November), DJF = winter (December, January, February).

Soil Moisture

Lowest mean pF values (corresponding to highest soil water tension) of 0–2 were measured in summer (JJAS) and autumn (ON), highest (corresponding to lowest soil water tension) of 2–5 were detected in winter (DJF), followed by spring months (AM 13, MAM) (Table 2). Overall, NE was higher by pF 0.4 than NW. On both transect, soils in the alpine tundra revealed year-round drier pF compared to lower altitudes (Table 2). Corresponding to ST measurements showing higher values in DJF 14/15 and MAM 15 compared to the previous year (DJF 13/14, MAM 14), we found distinctly lower pF values (corresponding to higher soil water tensions) in DJF 14/15 and MAM 15 (Table 2) on both transects.

A Kruskal Wallis test with post-hoc Nemenyi (Tukey) test of daily mean pF values (period: 01 May 2013–30 September 2015) on both altitudinal transects resulted in significant differences between zones ABC and D ($p < 0.0001$) (cf. Table 2). On NW, AB (0.38) did not vary significantly. On NE, AB (0.82) and AD (0.34) were similar, whereas AC, BC, BD, and CD ($p < 0.0001$) differed significantly from each other. The same tests for SM and AWC ended up in similar results. With regard to different seasons, we found a more complex spatial pattern of pF on NE than on NW (see results from post-hoc Nemenyi (Tukey) test in Table 2). However, zone D (alpine tundra) on both transects differed from the other zones nearly in every season.

Derived from pF values and soil texture (cf. Table 3), we calculated seasonal mean soil water content

TABLE 2

Mean (± s.e.) seasonal soil pF at 10 cm depth, and soil water content (SM) and available water capacity (AWC) in Vol.% or L m^{-2} dm^{-1} in the altitudinal zones A, B, C, and D on the NE and NW transect. AM 13 = April–May 2013, JJAS = summer (June, July, August, September), ON = autumn (October, November), DJF = winter (December, January, February), MAM = spring (March, April, May). Different letters indicate significant differences at $p < 0.05$ by Post-hoc Nemenyi (Tukey) test.

		Soil pF				SM (Vol.% or L $m^{-2}dm^{-1}$)				AWC (Vol.% or L $m^{-2}dm^{-1}$)			
Transect	Season	A	B	C	D	A	B	C	D	A	B	C	D
NE	AM 13 [1]	1.9 ± 0.9 ^{a}	1.9 ± 0.7 ^{b}	1.2 ± 0.1 ^{c}	2.2 ± 0.5 ^{d}	29.0 ± 4.0 ^{a}	27.3 ± 5.4 ^{b}	30.8 ± 1.5 ^{c}	17.1 ± 7.9 ^{d}	6.8 ± 1.3 ^{a}	6.0 ± 1.2 ^{b}	6.8 ± 0.6 ^{c}	3.6 ± 2.7 ^{d}
	JJAS 13	0.9 ± 0.8 ^{ac}	1.0 ± 0.7 ^{bc}	0.7 ± 0.5 ^{abc}	1.0 ± 0.4 ^{d}	35.6 ± 5.9 ^{ac}	34.5 ± 5.5 ^{bc}	35.3 ± 4.6 ^{abc}	29.9 ± 7.1 ^{d}	8.4 ± 1.8 ^{ac}	7.6 ± 1.2 ^{bc}	7.6 ± 1.1 ^{abc}	6.3 ± 1.6 ^{d}
	ON 13	1.7 ± 0.9 ^{a}	1.9 ± 1.6 ^{b}	1.6 ± 0.3 ^{c}	1.8 ± 0.9 ^{d}	28.6 ± 1.7 ^{a}	27.7 ± 5.6 ^{b}	28.9 ± 2.1 ^{c}	27.2± 8.8 ^{d}	6.7 ± 0.8 ^{a}	6.1 ± 2.5 ^{b}	5.8 ± 0.7 ^{c}	5.7 ± 1.8 ^{d}
	DJF 13/14	4.7 ± 0.7 ^{a}	4.2 ± 0.9 ^{b}	4.5 ± 0.6 ^{b}	4.7 ± 0.7 ^{a}	3.7 ± 4.4 ^{a}	7.8 ± 5.8 ^{b}	6.9 ± 4.8 ^{b}	3.4 ± 3.2 ^{a}	0.9 ± 1.1 ^{a}	1.7 ± 1.3 ^{a}	0.9 ± 1.1 ^{b}	0.7 ± 2.5 ^{b}
	MAM 14	2.6 ± 1.1 ^{a}	2.8 ± 1.1 ^{b}	2.0 ± 0.5 ^{b}	2.8 ± 0.9 ^{c}	19.5 ± 7.2 ^{a}	19.3 ± 5.5 ^{b}	25.4 ± 2.6 ^{b}	18.7 ± 8.7 ^{c}	4.5 ± 2.8 ^{a}	4.2 ± 1.2 ^{b}	5.2 ± 0.7 ^{b}	4.0 ± 2.0 ^{c}
	JJAS 14	1.3 ± 0.4 ^{a}	1.0 ± 0.7 ^{a}	0.9 ± 0.4 ^{a}	1.4 ± 0.4 ^{b}	31.4 ± 1.2 ^{a}	34.8 ± 5.5 ^{a}	34.8 ± 4.2 ^{a}	30.1 ± 2.3 ^{b}	7.4 ± 0.7 ^{a}	7.6 ± 1.2 ^{a}	7.4 ± 1.2 ^{a}	6.3 ± 0.6 ^{b}
	ON 14	1.3 ± 0.8 ^{a}	1.8 ± 0.3 ^{b}	1.2 ± 0.4 ^{c}	1.4 ± 0.8 ^{d}	32.4 ± 4.1 ^{a}	29.4 ± 2.3 ^{b}	30.8 ± 3.1 ^{c}	28.1 ± 7.3 ^{d}	7.7 ± 1.5 ^{a}	6.0 ± 0.5 ^{b}	6.6 ± 0.9 ^{c}	6.3 ± 1.9 ^{d}
	DJF 14/15	4.1 ± 0.9 ^{a}	3.5 ± 1.2 ^{b}	3.9 ± 0.5 ^{b}	4.1 ± 0.6 ^{a}	7.7 ± 7.0 ^{a}	14.2 ± 9.2 ^{b}	13.1 ± 3.4 ^{b}	7.1 ± 9.2 ^{a}	1.8 ± 1.8 ^{a}	3.1 ± 2.0 ^{b}	1.6 ± 0.8 ^{b}	1.2 ± 1.8 ^{a}
	MAM 15	2.5 ± 1.4 ^{a}	2.4 ± 1.2 ^{b}	1.7 ± 0.4 ^{b}	2.3 ± 0.6 ^{c}	24.2 ± 3.8 ^{a}	24.3 ± 7.3 ^{b}	28.0 ± 1.9 ^{b}	23.7 ± 5.0 ^{c}	5.7 ± 0.9 ^{a}	5.3 ± 1.6 ^{b}	5.7 ± 0.4 ^{b}	5.0 ± 1.0 ^{c}
	JJAS 15	1.4 ± 0.8 ^{a}	1.7 ± 0.6 ^{b}	0.9 ± 0.4 ^{a}	1.8 ± 0.8 ^{c}	29.5 ± 3.3 ^{a}	29.4 ± 3.6 ^{b}	30.2 ± 3.5 ^{a}	27.0 ± 2.7 ^{c}	6.9 ± 0.7 ^{a}	6.5 ± 0.8 ^{b}	7.3 ± 1.0 ^{a}	5.7 ± 0.6 ^{c}
NW	AM 13[1]	1.1 ± 0.2 ^{a}	1.3 ± 0.2 ^{b}	1.2 ± 0.1 ^{c}	1.5 ± 0.1 ^{d}	32.9 ± 3.5 ^{a}	32.3 ± 1.7 ^{b}	32.3 ± 1.1 ^{c}	30.2 ± 1.7 ^{d}	7.8± 1.3 ^{a}	7.1 ± 0.4 ^{b}	7.0 ± 0.9 ^{c}	6.6 ± 1.0 ^{d}
	JJAS 13	0.9 ± 0.4 ^{ab}	0.9 ± 0.4 ^{bc}	0.9 ± 0.4 ^{bc}	1.4 ± 0.2 ^{d}	35.9 ± 3.6 ^{ab}	35.3 ± 3.4 ^{bc}	35.1 ± 3.5 ^{bc}	31.1 ± 1.8 ^{d}	8.5 ± 1. 4 ^{ab}	7.8 ± 0.7 ^{bc}	7.7 ± 1.3 ^{bc}	6.8 ± 1.0 ^{d}
	ON 13	1.1 ± 0.7 ^{a}	1.3 ± 0.5 ^{b}	1.5 ± 0.6 ^{c}	1.8 ± 0.4 ^{d}	34.0 ± 5.0 ^{a}	32.3 ± 0.8 ^{b}	29.8 ± 4.6 ^{c}	26.7 ± 1.8 ^{d}	8.0 ± 1.6 ^{a}	7.1 ± 0.2 ^{b}	6.5 ± 1.2 ^{c}	5.8 ± 0.4 ^{d}
	DJF 13/14	3.9 ± 1.3 ^{a}	4.0 ± 0.5 ^{b}	4.4 ± 0.7 ^{c}	4.9 ± 0.8 ^{d}	11.1 ± 7.8 ^{a}	8.4 ± 2.8 ^{b}	4.4 ± 4.6 ^{c}	1.6 ± 3.0 ^{d}	2.6 ± 1.9 ^{a}	1.9 ± 0.6 ^{b}	1.0 ± 1.0 ^{c}	0.3 ± 0.6 ^{d}
	MAM 14	1.7 ± 0.9 ^{a}	1.9 ± 0.2 ^{b}	2.1 ± 0.4 ^{c}	2.2 ± 0.7 ^{d}	28.6 ± 5.1 ^{a}	27.2 ± 0.9 ^{b}	24.2 ± 3.1 ^{c}	23.0 ± 3.7 ^{d}	6.8 ± 1.6 ^{a}	6.0 ± 0.2 ^{b}	5.3 ± 1.1 ^{c}	4.9 ± 0.4 ^{d}
	JJAS 14	0.7 ± 0.5 ^{a}	1.0 ± 0.2 ^{b}	0.7 ± 0.5 ^{b}	1.0 ± 0.4 ^{c}	38.0 ± 4.3 ^{a}	34.0 ± 2.5 ^{b}	36.7 ± 4.5 ^{b}	33.2 ± 2.3 ^{c}	9.0 ± 1.6 ^{a}	7.5 ± 0.6 ^{b}	8.0 ± 1.8 ^{b}	7.2 ± 1.0 ^{c}
	ON 14	1.0 ± 0.6 ^{a}	0.5 ± 0.7 ^{b}	1.1 ± 0.5 ^{c}	1.6 ± 0.4 ^{d}	35.5 ± 2.3 ^{a}	39.5 ± 4.6 ^{b}	33.2 ± 3.8 ^{c}	28.7 ± 1.4 ^{d}	8.3 ± 0.9 ^{a}	8.7 ± 1.0 ^{b}	7.3 ± 1.5 ^{c}	6.2 ± 0.9 ^{d}
	DJF 14/15	2.7 ± 1.1 ^{a}	1.6 ± 1.8 ^{a}	3.1 ± 1.1 ^{b}	3.1 ± 0.6 ^{c}	19.1 ± 9.5 ^{a}	29.0 ± 9.3 ^{a}	14.6 ± 7.1 ^{b}	13.6 ± 5.6 ^{c}	4.4 ± 2.0 ^{a}	6.4 ± 2.2 ^{a}	3.1 ± 2.1 ^{b}	3.0 ± 1.2 ^{c}
	MAM 15	1.3 ± 0.6 ^{a}	1.2 ± 0.8 ^{b}	1.8 ± 0.3 ^{c}	1.8 ± 0.3 ^{d}	32.1 ± 2.6 ^{a}	29.8 ± 7.3 ^{b}	27.1 ± 0.8 ^{c}	26.9 ± 1.1 ^{d}	7.6 ± 0.8 ^{a}	6.6 ± 1.6 ^{b}	5.9 ± 0.7 ^{c}	5.8 ± 0.7 ^{d}
	JJAS 15	0.9 ± 0.5 ^{a}	1.2 ± 0.7 ^{b}	1.2 ± 0.6 ^{c}	1.7 ± 0.3 ^{d}	36.2 ± 3.9 ^{a}	28.9 ± 7.4 ^{b}	33.0 ± 6.2 ^{c}	27.4 ± 3.0 ^{d}	8.6 ± 1.5 ^{a}	6.4 ± 1.6 ^{b}	7.3 ± 2.2 ^{c}	6.0 ± 1.0 ^{d}

[1] Data in April are available from 18 April 2013.

TABLE 3

Summary of vegetation, soil texture, and bulk density data (means of altitudinal zones ± s.e.). Soil texture and bulk density were used for calculation of soil moisture (SM) and available water capacity (AWC) at 0–10 cm soil depth. dbh = diameter at breast height. NE = northeast, NW = northwest. A, B, C, D = altitudinal zones. Different letters indicate significant differences at $p < 0.05$ by Post-hoc Nemenyi (Tukey) test.

Transect—Altitudinal zone	Tree height (m)	Crown width (m)	Crown length (m)	dbh (cm)	Individuals (dbh ≥ 7 cm) (*n*)	Leaf area index (LAI)	Sand (%)	Silt (%)	Clay (%)	Bulk density (g cm^{-3})
NE—A	7.84 ± 1.13 ^{a}	4.24 ± 0.33 ^{a}	4.08 ± 0.74 ^{a}	16.59 ± 2.13 ^{a}	50 ± 18 ^{a}	1.74 ± 0.17 ^{a}	65 ± 2 ^{a}	27 ± 1 ^{a}	8 ± 2 ^{a}	1.24 ± 0.17 ^{a}
NE—B	5.66 ± 0.52 ^{a}	3.61 ± 0.36 ^{a}	3.08 ± 0.28 ^{a}	14.02 ± 0.72 ^{a}	96 ± 23 ^{b}	1.88 ± 0.22 ^{a}	63 ± 4 ^{a}	28± 2 ^{a}	9 ± 1 ^{a}	1.14 ± 0.09 ^{ab}
NE—C	1.94 ± 0.86 ^{b}	2.35 ± 0.13 ^{b}	0.82 ± 0.22 ^{b}	7.90 ± 0.44 ^{b}	40 ± 36 ^{a}	1.47 ± 0.14 ^{a}	68 ± 5 ^{a}	24 ± 4 ^{a}	8 ± 1 ^{a}	1.10 ± 0.11 ^{a}
NE—D	0.55 ± 1.10 ^{c}	0.38 ± 0.75 ^{c}	0.31 ± 0.63 ^{c}	1.83 ± 3.65 ^{c}	1 ± 1 ^{c}	0.14 ± 0.07 ^{b}	73 ± 6 ^{a}	19 ± 5 ^{a}	8 ± 3 ^{a}	0.97 ± 0.01 ^{b}
NW—A	5.64 ± 0.34 ^{a}	3.58 ± 0.53 ^{a}	3.24 ± 0.20 ^{a}	11.62 ± 1.86 ^{a}	42 ± 19 ^{a}	1.49 ± 0.16 ^{a}	65 ± 1 ^{a}	27 ± 1 ^{a}	8 ± 1 ^{a}	1.20 ± 0.17 ^{a}
NW—B	5.46 ± 0.74 ^{a}	4.03 ± 1.06 ^{a}	3.35 ± 0.85 ^{a}	13.90 ± 2.04 ^{a}	45 ± 13 ^{a}	1.35 ± 0.13 ^{a}	61 ± 1 ^{a}	30 ± 2 ^{a}	9 ± 1 ^{a}	1.38 ± 0.08 ^{a}
NW—C	2.47 ± 0.38 ^{b}	2.26 ± 0.15 ^{b}	1.10 ± 0.36 ^{b}	8.63 ± 0.68 ^{b}	105 ± 60 ^{b}	1.27 ± 0.27 ^{a}	69 ± 7 ^{a}	24 ± 6 ^{a}	7 ± 2 ^{a}	1.20 ± 0.14 ^{a}
NW—D	0.53 ± 1.05 ^{c}	0.28 ± 0.56 ^{c}	0.25 ± 0.50 ^{c}	1.78 ± 3.55 ^{c}	1 ± 2 ^{c}	0.11 ± 0.02 ^{b}	69 ± 7 ^{a}	23 ± 5 ^{a}	8 ± 2 ^{a}	1.07 ± 0.11 ^{a}

(SM, in Vol.-% or L m^{-2}dm^{-1}, 0–10 cm soil depth, Table 2). According to IUSS (2006), soil texture at 10 cm depth is sand or loamy sand. Further, available water capacity (AWC, Vol.-% or L m^{-2}dm^{-1}, 0–10 cm soil depth, Table 2, Fig. 5) was calculated from SM, texture, and bulk density (cf. Table 3). Likewise to pF, highest SM and AWC, respectively, were calculated for summer (JJAS), followed by autumn (ON), spring (MAM), and winter (DJF) (cf. Fig. 5). Both transects had year-round lowest SM and AWC in the alpine tundra (D) (Table 2). For the period from 1 May 2013 to 30 September 2015, we calculated a decline of mean AWC from A to D on both transects (NE: A = 5.53, B = 5.39, C = 5.51, D = 5.20, NW: A = 7.13, B = 6.69, C = 5.92, D = 5.40).

Stand Structure and Tree Physiognomy

For multivariate statistical analyses, we used tree physiognomy data from each experimental plot, which has been described previously in detail in Schwab et al. (2016). Thus, merely a brief summary of the data is presented as means of altitudinal zones (± standard error) in Table 3. Tree height, crown width, crown length, and dbh decreased with elevation. Crown width, crown length, and dbh, respectively, were higher in the uppermost closed forest (B) than in the closed forest (A) on NW. On NE, the uppermost closed forest (B) showed the highest number of tree individuals (dbh ≥ 7 cm), whereas on NW most individuals occurred in krummholz (C). LAI was similar in A and B, and decreased at the transition from B to C, more notable on NE. LAI declined sharply in the alpine tundra (D) on both transects. In general, all investigated vegetation variables indicate higher values on NE.

In Table 3, we also included results from soil texture and soil bulk density. Soil texture is commonly very homogeneous throughout the study area with generally coarse grain sizes (proportion of sand > 60%). Bulk density is overall low across the alpine treeline ecotone (~1 g cm^{-3}), with marginal differences between altitudinal zones (Table 3).

Multivariate Statistics

In a first step, a PCA including the different ST variables resulted in 70% proportion of variance for

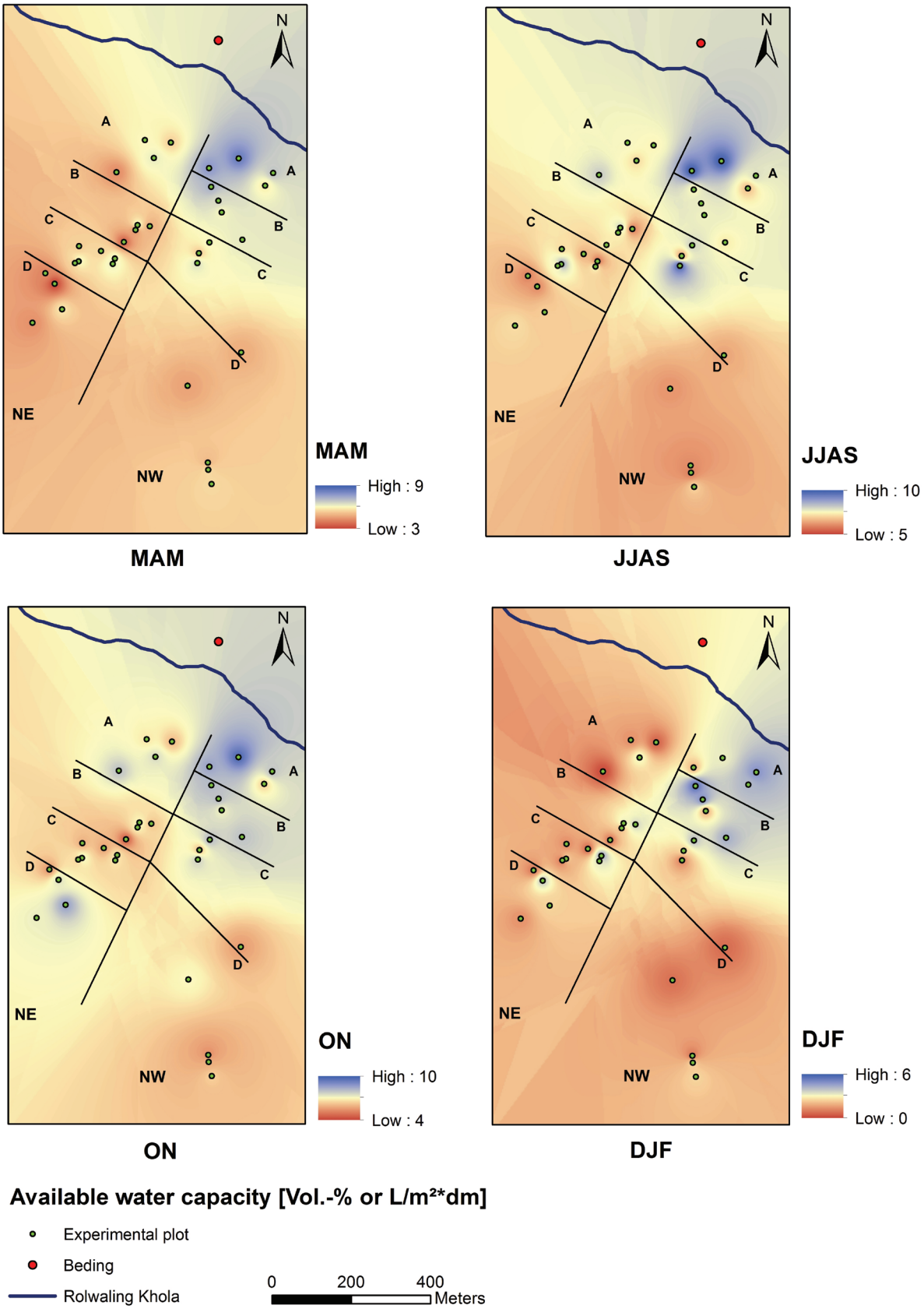

FIGURE 5. Spatiotemporal variation in available water capacity (Vol.% or L $m^{-2}dm^{-1}$). A, B, C, D = altitudinal zones. NW = northwest. NE = northeast. MAM = March–May, JJAS = June–September, ON = October–November, DJF = December–February.

principal component 1 (PC1), which was represented predominantly by the STs measured in the entire period (01 May 2013–31 October 2015), and in spring 2014 (MAM 14) and 2015 (MAM 15), respectively. A 19% proportion of variance was explained by principal component 2 (PC2), which included primarily spring temperatures in 2013 (AM 13), and winter temperatures (DJF 13/14, 14/15).

The same method applied to AWC revealed 50% proportion of variance for PC1 (entire period, summer [JJAS]), and 31% for PC2, mainly covered by winter (DJF), and spring (AM 13, MAM). A PCA of SM led to 40% proportion of variance by PC1, including the entire period, spring, and summer. PC2 (34%) was composed primarily of winter SM (DJF).

We integrated the different PCs (summarized as ST and AWC) as vector variables into a redundancy analysis (RDA) to test their relations to the dependent variables (cf. Table 3). Figure 6 indicates that ST is the most important independent variable on the first axis (RDA1), and that AWC is most important on the second axis (RDA2). The proportion explained by the RDA 1 axis was 99%, while the RDA 2 axis represented 1%. ST was strongly correlated with crown length and tree height. LAI, crown width, dbh, and the number of tree individuals correlated less strongly with both ST and AWC (Fig. 6).

The circles (Fig. 6, part a) indicate diverse groups representing differences among the altitudinal zones. Zones A and B (closed forest, A = green, B = brown) overlap partially, whereas C (krummholz, gray), and D (alpine tundra, black) provide individual groups showing a small overlap only (confidence interval = 0.95). The groups imply a very homogeneous distribution of sites, especially the group of sites D where six sites are virtually equal (black dots in the upper left corner of Fig. 6, part a). With regard to exposition, no major differences occur between the sites of the altitudinal transects NE and NW (Fig. 6, part b).

A summary of the RDA using the *RsquareAdj* function in R showed that the proportion of the total variance explained by the independent variables is 16.5%. We used the same function to see the variation explained by the individual independent variables. Hereafter, the conditional effect of ST on the dependent variables was highest (6.9%), followed by AWC (3.7%). The shared variation of the two variables was 5.9%. An ANOVA of the RDA results returned a Monte Carlo permutation test of the predictor effect, which was significant ($p = 0.01$).

To verify these results, and to explain the effects of each independent variable on the individual dependent variables in more detail, we separately applied a multivariate linear regression analysis with ensuing MANOVA. The results (Table 4, part a) show that the variances of the dependent variables LAI, crown width, crown length, and tree height are best explained by ST at a significance level of $p = 0.05$, respectively. In summary, our model for multivariate linear regression (after MANOVA) was significant for ST only ($p = 0.04$).

Figure 7 illustrates the linear relationships between ST and AWC, and relevant dependent variables (tree height, crown length) with regard to exposition (NE, NW). STs were found to be significantly positive related to both tree height and crown length on NE and NW, respectively. AWC was significantly positive related to tree height on NW. No significant relations were detected between AWC and crown length (Fig. 7).

In turn, we also tested the relations between various environmental variables and the dependent variables ST, AWC, and SM with multivariate linear regression analyses. The results indicate that all three dependent variables together are best predicted by elevation ($p = 0.002$), and tree height ($p < 0.01$), where elevation explained 79% of the variance in tree height. With regard to each individual dependent variable (Table 4, part b) the results were similar. Our model for the explanation of ST fitted best for tree height with an adjusted R^2 of the model of 13% (significant, $p = 0.02$). AWC was more related to elevation and tree height, respectively (adj. $R^2 = 44\%$, $p < 0.001$). The results for SM looked similar, with the independent variables elevation, tree height, and number of tree individuals creating the best-fitting model (adj. $R^2 = 38\%$, $p < 0.001$). Neither soil-related independent variables (texture, bulk density, thickness of litter layer) nor aspect improved the models.

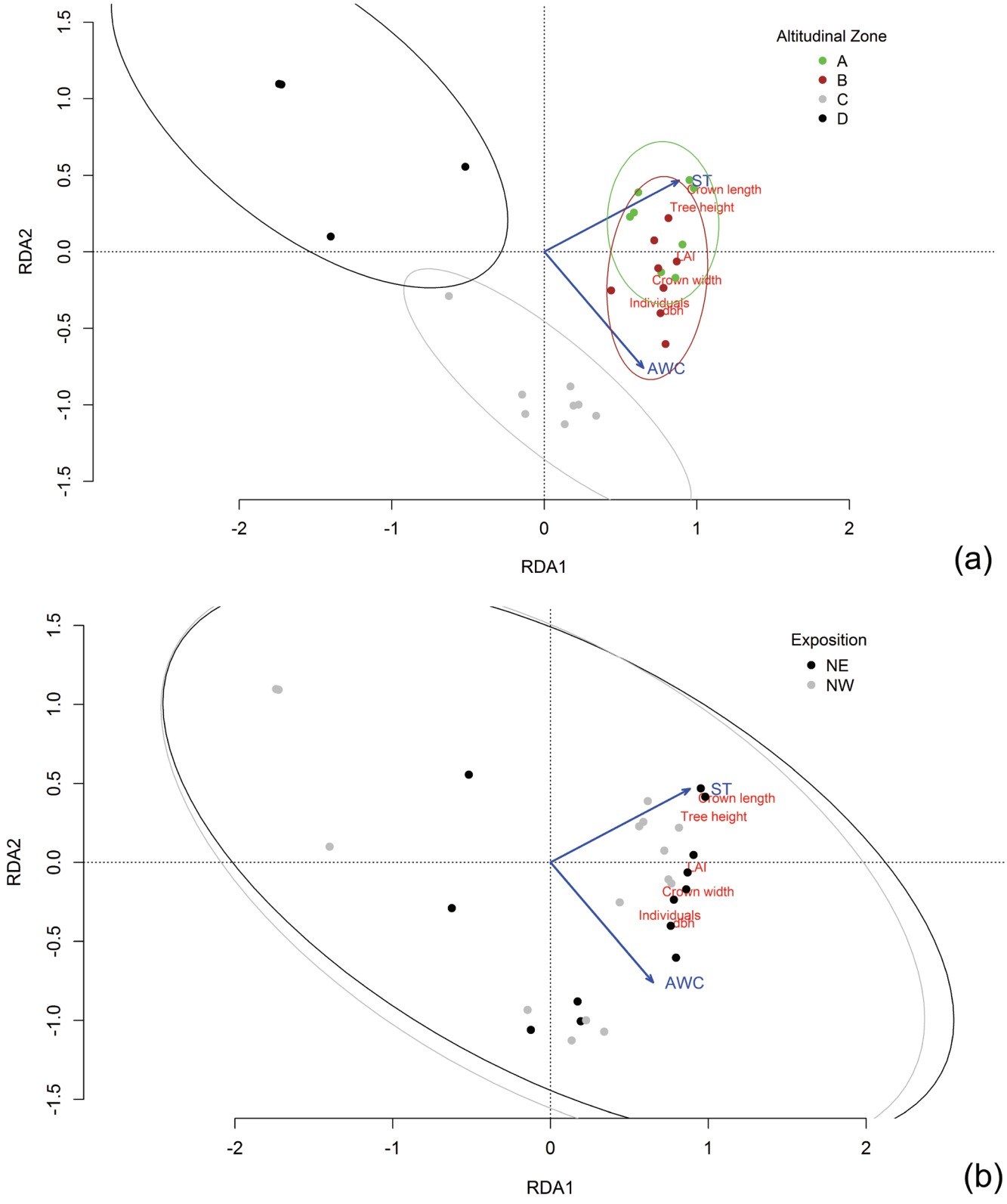

FIGURE 6. Results from redundancy analysis (RDA) with regard to (a) altitudinal zones, and (b) exposition. Blue arrows represent the independent explanatory variables soil temperature (ST), and available water capacity (AWC) gained as best explained principal components from preceding principal component analysis (PCA). The dependent response variables diameter in breast height (dbh), leaf area index (LAI), tree height, crown width, crown length, and number of tree individuals (Individuals) are colored in red. Circles combine related groups of sites (NE = northeast, NW = northwest. A, B, C, D = altitudinal zones). Scaling = 2 (in programming language R).

TABLE 4

Results of multivariate linear regression analyses. (a) The *t* and *p* values (*T*-test) are presented for relationships between explanatory variables (ST [soil temperature], AWC), and response variables. The explanation of the response variables is significant at a significance level of $p = 0.05$. (b) The best model for explanation of the response variables (ST, AWC, SM [soil moisture]) was produced by stepwise selection of independent variables. The results are highly significant at a significance level of $p = 0.001$ and $p = 0.01$, and significant at $p = 0.05$. LAI = leaf area index, dbh = diameter in breast height.

(a)	LAI		dbh		Tree height		Crown length		Crown width		Tree individuals	
	t	*p*	*t*	*p*	*t*	*p*	*t*	*p*	*t*	*p*	*t*	*p*
ST	1.72	0.05*	1.37	0.18	2.13	0.04*	2.56	0.02*	1.66	0.05*	1.21	0.24
AWC	1.09	0.29	1.21	0.24	1.02	0.32	1.15	0.26	1.20	0.24	1.07	0.30

(b)	ST				AWC				SM		
	t	*p*	Adj. R^2		*t*	*p*	Adj. R^2		*t*	*p*	Adj. R^2
Tree height	2.38	0.02*	0.13	Elevation	4.74	<0.001***	0.44	Elevation	4.40	<0.001***	0.38
				Tree height	3.40	0.002**		Tree height	3.85	<0.001***	
								Individuals	1.96	0.05*	

Significance codes: 0.001 "***," 0.01 "**," 0.05 "*." 0.1 '.'

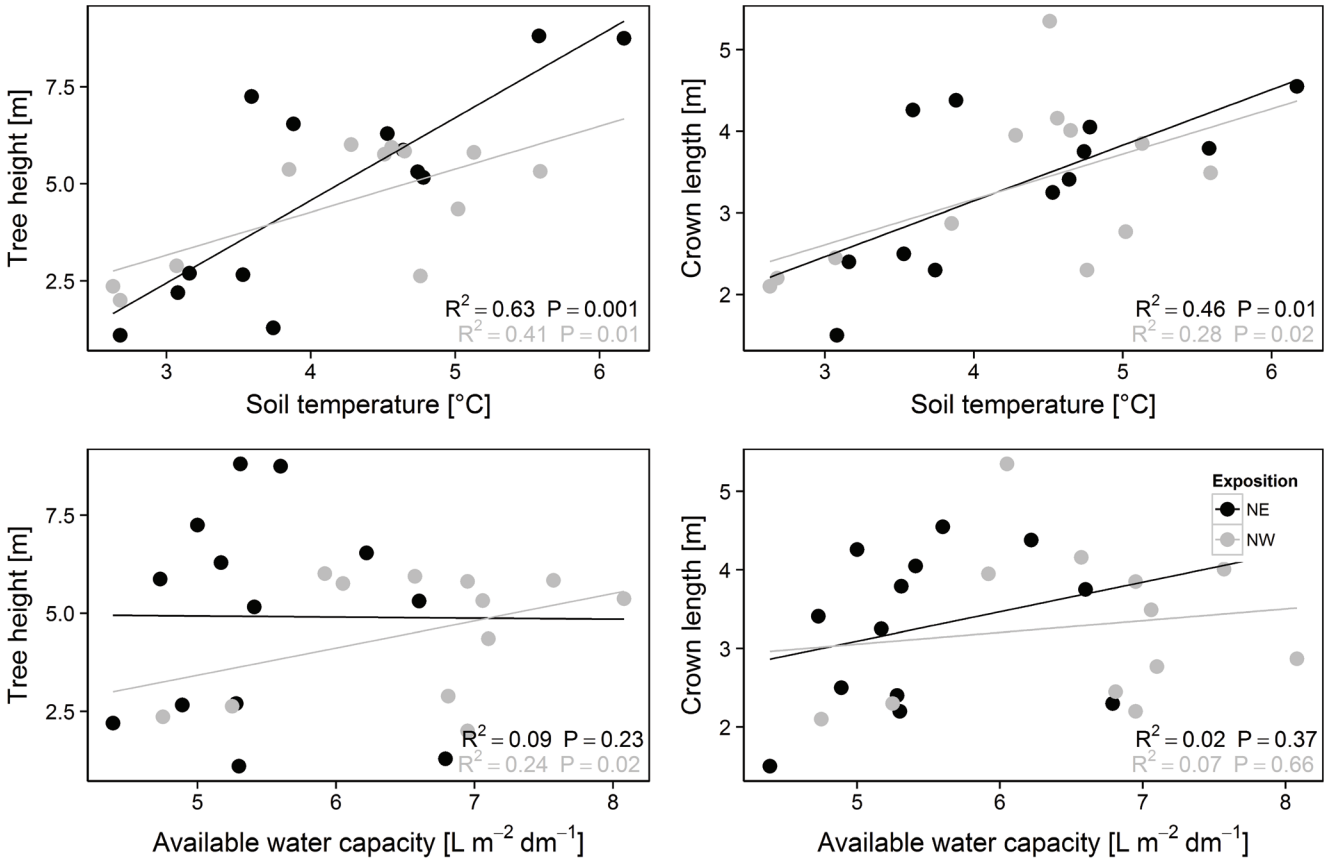

FIGURE 7. Scatter plot matrices showing simple linear regressions (R^2, *P*-value) between soil temperature (ST) and available water capacity (AWC), respectively, and tree height and crown length, respectively, with regard to exposition. NE = northeast, NW = northwest, m = meter, L m^{-2} dm^{-1} = liter per square meter per decimeter.

Discussion

ST is expected to be the second most important factor controlling tree growth at its upper limit both at global and local scales (Müller et al., 2016), and multivariate statistical analyses in Rolwaling imply a significant interaction between ST and vegetation patterns as well. In fact, STs in Rolwaling indicate a significant decline with elevation, and hereby especially at the transition from the uppermost closed forest (B) to krummholz (C) (equal to timberline and treeline in this case). The reason why our statistical analyses did not result in a significant relation between STs and elevation (cf. Table 4, part b) is because year-round higher STs in the alpine tundra compared to krummholz on NE (cf. Fig. 4, Table 1). This suggests a stronger influence of solar radiation in this zone and points to the effect of dense canopies preventing soil heat flux and radiative warming, particularly underneath krummholz (cf. Aulitzky, 1961; Körner, 1998a, 1998b; Körner and Paulsen, 2004). Differences in the canopy cover are confirmed by substantially higher LAI values in the krummholz zone than in the alpine tundra (Table 3). This was also found on NW, where the canopy was generally less dense (lower LAI) compared to NE along the entire transect (Table 3). However, we found different ST patterns on NW, where STs in the alpine tundra were generally lowest compared to lower elevation throughout the entire measurement period, except for autumn 2013 and winter 2013/2014. This suggests that—despite a less dense canopy on NW—the influence of solar radiation is lower than on NE. Since mean STs at treeline during growing seasons in 2013, 2014, and 2015 were slightly higher or the same on NW than on NE (cf. Fig. 3)—despite a lower elevation of treeline of ~100 m—we assume that STs alone are not responsible for the elevational position of the treeline in the study area. Moreover, the higher growing season mean ST at treeline of 7.5 ± 0.6 °C compared to a suggested global mean of 6.4 ± 0.7 °C (Körner, 2012) may indicate that a combination of different factors (e.g., soil water availability, soil nutrient availability) limit tree growth (e.g., Leuschner, 1996; Harsch and Bader, 2011). It has been suggested that warmer treelines are governed by seedling survival rather than growth (cf. Harsch and Bader, 2011), since seedlings are said to depend strongly on water and nutrient availability, frost damage, or are intolerant to sun exposure (Ball et al., 1991; Germino et al., 2002; Gieger and Leuschner, 2004; Holtmeier and Broll, 2005, 2007; Smith et al., 2009). However, a ~100 m higher position of uppermost trees on NE suggests that STs favor tree growth depending on the exposition. A higher solar radiation load finds expression in seasonal higher STs, and thus in higher trees, a thicker dbh, and a higher LAI on NE (cf. Tables 1 and 3). Nevertheless, exposition as independent variable does not explain ST patterns in our statistical analyses. Also, simple linear regression analyses show no major differences in the relationships between ST, and relevant vegetation variables (tree height, crown length) with regard to the exposition (Fig. 7). Overall, our results reveal a complex microclimatic pattern of STs, which may be caused by topography-induced higher solar radiation load, and thus higher STs, and also by the vegetation pattern itself, which influences soil climatic conditions inside and outside of the closed forest and krummholz in different ways by shading effects and variation in leaf fall.

In contrast, the results of multivariate analyses do not show a significant impact of AWC (0–10 cm soil depth) on vegetation patterns (cf. Table 4, part a). In turn, SM and AWC are likely controlled by tree height and elevation (Table 4, part b; cf. Fig. 7), and AWC is additionally related to the number of tree individuals (Table 4, part b). Since elevation and/or altitude as environmental variable cannot explain differences in soil moisture (Körner, 2012), we do not attach too much importance to elevation as explanatory factor for SM and AWC in this analysis. Moreover, SM and AWC are controlled by the stand structure and the tree physiognomy themselves. Year-round lowest AWC in the alpine tundra on both transects (cf. Fig. 5, Table 2) is most likely critical in preventing seedlings from invading such sites. In the study area, Schickhoff et al. (2015) found the abundance of young growth from species *Abies spectabilis*, *Betula utilis*, and *Rhododendron campanulatum* over almost all size classes to be significantly correlated to SM. The main reasons for overall low water-holding capacities of soils in the study area are rapidly draining sandy substrates (cf. Table 3), low bulk densities (~1 g cm^{-3}, cf. Table 3), and a large amount of skeleton (up to 95%), and thus a pronounced water percolation from topsoil

to subsoil. This process is evidenced by well-shaped horizontal structures of soils, marked by thick (up to 30 cm) ash-gray eluvial horizons (Ae), and illuvial horizons (Bh, Bs) in the subsoil. These structures result from a soil downward dislocation of soil organic matter, and sesquioxides (e.g., Al, Fe) with percolating water (podzolisation). In the alpine tundra, SM conditions and also water potential in plants are both most likely additionally affected by evapotranspiration provoked by a stronger influence of both solar radiation and wind compared to forest and krummholz sites, resulting in an enhanced drying of topsoils and plants. Compared to forest sites, desiccation of topsoils through solar radiation and wind is strengthened by a less developed organic layer (litter layer < 0.5 cm) (cf. Wardle, 1968; Doležal and Šrutek, 2002). Likewise, tree regeneration has been observed as being strongly hindered by excessive solar radiation and water stress at treelines worldwide (Aulitzky, 1960, 1961; Ferrar et al., 1988; Ball et al., 1991; Bader et al., 2007; Danby and Hik, 2007; Gill et al., 2015; Moyes et al., 2015). Overall, we assume seedling establishment in the alpine tundra in early life stages to be likely modified by SM availability, and to depend on protection from excessive solar radiation by other small growing plants (dwarf shrubs), and by topographical shelters (e.g., large rocks). Likewise, a different study in the Himalaya (Manang Valley) from Shrestha (2007) showed that regeneration of *Betula utilis* is constrained by SM availability and canopy cover (light), respectively. In the same study area, *Abies spectabilis* seedling abundance has been observed to depend on SM availability and nutrients (phosphorus), respectively (Ghimire and Lekhak, 2007). Previous studies from Rolwaling indicate a significant decline of soil nutrients (e.g., nitrogen, phosphorus) along the altitudinal transects, which has been interpreted as low soil nutrient availability being a most likely limiting factor for tree growth even well below the climatic treeline (Müller et al., 2016). Nutrient uptake by plants may be further affected by limited SM supply as found for other treelines as well (Loomis et al., 2006; Macek et al., 2012).

Moreover, SM is affected by low STs indirectly through freezing of soil water in the study area, predominantly in winter and spring (cf. Dong et al., 2011). Soils across the alpine treeline ecotone were frozen from October 2013 at least until end of April 2014. Higher STs (around 0 °C), and higher SM and AWC in winter 2014/2015 and spring 2015 compared to the same seasons in the previous year, suggest a thicker snowpack during these seasons. This conclusion is derived from findings that a greater snow depth usually induces warmer soils (Holtmeier and Broll, 2007, 2010; Wieser and Tausz, 2007; Hagedorn et al., 2014), leading to consistent STs around 0 °C (Green, 1983; Holtmeier, 2005, 2009; Stöhr, 2007; Shi et al., 2008). In the Ural Mountains, a thicker snow cover in winter, and thus warmer soils, were found to be more important for tree growth and treeline advance than summer temperatures (Hagedorn et al., 2014). Further, a higher snow cover keeps SM high also during winter, and protects soils from frost, and small plants (dwarf scrubs and seedlings) from cold temperatures, evapotranspiration, and damage by high solar radiation and wind. In turn, a missing or thin snow cover may induce deep soil freezing (Wieser and Tausz, 2007). Thus, frost drought due to frozen soils, and mechanical damage, have been assumed to be limiting for tree growth, especially during winter months, when water uptake by plants is impeded (Larcher, 1957, 1963; Kupfer and Cairns, 1996; Oberhuber, 2004; Holtmeier, 2005; Mayr et al., 2006; Kullman, 2007). The issue of frost drought is supported by our data from winter 2013/2014, and partly spring 2014 (March, April), when both STs (<0 °C) and SM were low. In contrast, winter desiccation has been negated as a cause for treeline formation (e.g., Troll, 1961; Slatyer, 1976; Körner, 1998a, 2009; Richardson and Friedland, 2009). However, late winter, and in particular spring water losses were observed not being replaced due to frozen soils and stem bases (Körner, 1998a), leading to damage of leaves/needles and branches. In the study area, winter and premonsoonal drought stress—in case a sufficient snow cover is missing—may not only be a problem under canopies but also in the alpine tundra, resulting in impeded tree growth and regeneration. This has been observed for several other Himalayan treelines (Schickhoff et al., 2015). It has been suggested that constraints on tree growth due to warming-related drought stress may nullify any beneficial effect on alpine treelines due to rising temperatures (González de Andrés et al., 2015).

In summary, our results show that monitoring and analyzing spatiotemporal ST and SM data over a longer period of time is valuable for a distinction of ST and SM patterns between different topographic settings, different seasons, and different years, respectively. Considering ST and SM conditions during growing season only is insufficient to understand the complex mechanisms determining the interactions between ST and SM, topography, and vegetation patterns in an alpine treeline ecotone at local scales. This paper suggests an interaction of different factors (soil temperature, soil water availability, snow cover, wind, topography-induced solar radiation, vegetation, soil nutrient availability) to be responsible for tree growth and regeneration of trees in Rolwaling.

Conclusions

Our results indicate a strong interaction between STs, SM, and vegetation patterns (closed forest and krummholz vs. alpine tundra) in the Rolwaling treeline ecotone. We assume SM patterns to depend on alterations in snow cover, and to modify current and potential future vegetation patterns. Year-round lowest AWCs in soils of the alpine tundra are likely caused by a higher influence of solar radiation and wind compared to canopy-covered sites. We suggest seasonal drought stress in combination with nutrient-poor soils as critical factors constraining regeneration, and thus tree growth even well below the climatic treeline. Our results further show the importance of a long-term monitoring from ST and SM to determine seasonal varying soil conditions and their individual impact on vegetation patterns, tree growth, and regeneration, and vice versa. With regard to the Himalaya, more studies are needed with focus on SM conditions prior to the vegetation period.

Acknowledgments

This study was carried out in the framework of the TREELINE project and funded by the German Research Foundation (DFG SCHO 739/14-1, SCHI 436/14-1, BO 1333/4-1). We would like to thank Ram Bahadur, Björn Bonnet, Lena Geiger, Helge Heyken, Agnes Krettek, and Ronja Wedegärtner for their support. We also express our gratitude to Nepalese authorities for research permits, and to several local people in Beding who provided lodging and support in field data collection.

References Cited

Ad-hoc-Arbeitsgruppe Boden, 2005: *Bodenkundliche Kartieranleitung. Bundesanstalt für Geowissenschaften und Rohstoffe*. Hannover, Germany: Schweizerbart, 438 pp.

Aulitzky, H., 1960: Die Bodentemperaturverhältnisse an einer zentralalpinen Hanglage beiderseits der Waldgrenze. *Archiv für Meteorologie, Geophysik und Bioklimatologie*, Serie B 10(4): 445–532.

Aulitzky, H., 1961: Die Bodentemperaturverhältnisse in der Kampfzone oberhalb der Waldgrenze und im subalpinen Zirben-Lärchenwald. *Mitteilungen der Forstlichen Bundesversuchsanstalt Mariabrunn*, 59: 153–208.

Bader, M. Y., van Geloof, I., and Rietkerk, M., 2007: High solar radiation hinders tree regeneration above the alpine treeline in northern Ecuador. *Plant Ecology*, 191(1): 33–45.

Balducci, L., Deslauriers, A., Giovannelli, A., Rossi, S., and Rathgeber, C. B. K., 2013: Effects of temperature and water deficit on cambial activity and woody ring features in *Picea mariana* saplings. *Tree Physiology*, 33: 1006–1017.

Ball, M. C., Hodges ,V. S., and Laughlin, G. P., 1991: Cold-induced photoinhibition limits regeneration of Snow Gum at tree-line. *Functional Ecology*, 5(5): 663–668.

Biondi, F., 2001: A 400-year tree-ring chronology from the tropical treeline of North America. *AMBIO*, 30(3): 162–166.

Blume, H. P., Stahr, K., and Leinweber, P., 2011: *Bodenkundliches Praktikum: Eine Einführung in pedologisches Arbeiten für Ökologen, insbesondere Land- und Forstwirte, und für Geowissenschaftler*. 3. Aufl. Heidelberg: Spektrum Akademischer Verlag, 255 pp.

Camarero, J. J., and Gutiérrez, E., 2004: Pace and pattern of recent treeline dynamics: response of ecotones to climatic variability in the Spanish Pyrenees. *Climate Change*, 63: 181–200.

Danby, R. K., and Hik, D. S., 2007: Responses of white spruce (*Picea glauca*) to experimental warming at a subarctic alpine treeline. *Global Change Biology*, 13(2): 437–451.

Daniels, L. D., and Veblen, T. T., 2004: Spatiotemporal influences of climate on altitudinal treeline in northern Patagonia. *Ecology*, 85(5): 1284–1296.

Doležal, J., and Šrutek, M., 2002: Altitudinal changes in composition and structure of mountain-temperate vegetation: a case study from the Western Carpathians. *Plant Ecology*, 158: 201–221.

Dong, M., Jiang, Y., Zhang, W., Yang, Y., and Yang, H., 2011: Effect of alpine treeline conditions on the response of the stem radial variation of *Picea meyeri rebd. et wils* to environmental factors. *Polish Journal of Ecology*, 59(4): 729–739.

Ferrar, P. J., Cochrane, P. M., and Slatyer, O., 1988: Factors influencing germination and establishment of *Eucalyptus pauciflora* near the alpine tree line. *Tree Physiology*, 4: 27–43.

Fox, J., and Weisberg, S., 2011: An R companion to applied regression. 2nd edition. *Sage*, http://socserv.socsci.mcmaster.ca/jfox/Books/Companion, accessed 6 January 2016.

Germino, M. J., Smith, W. K., and Resor, A. C., 2002: Conifer seedling distribution and survival in an alpine-treeline ecotone. *Plant Ecology*, 162: 157–168.

Ghimire, B. K., and Lekhak, H. D., 2007: Regeneration of *Abies spectabilis* (D. Don) Mirb. in subalpine forest of upper Manang, north-central Nepal. *In* Chaudhary, R. P., Aase, T. H., Vetaas,. O, and Subedi, B. P. (eds.), *Local Effects of Global Changes in the Himalayas: Manang, Nepal*. Tribhuvan University, Nepal, and University of Bergen, Norway, 139–149.

Gieger, T., and Leuschner, C., 2004: Altitudinal change in needle water relations of *Pinus canariensis* and possible evidence of a drought-induced alpine timberline on Mt. Teide, Tenerife. *Flora—Morphology, Distribution, Functional Ecology of Plants*, 199(2): 100–109.

Gill, R. A., Campbell, C. S., and Karlinsey, S. M., 2015: Soil moisture controls Engelmann spruce (*Picea engelmannii*) seedling carbon balance and survivorship at timberline in Utah, USA. *Canadian Journal of Forest Research, 45*(12): 1845–1852.

González de Andrés, E., Camarero, J. J., and Büntgen, U., 2015: Complex climate constraints of upper treeline formation in the Pyrenees. *Trees, 29*(3): 941–952.

Green, F. H. W., 1983: Soil temperature and the tree line: a note. *Scottish Geographical Magazine*, 99(1): 44–47.

Hagedorn, F, Shiyatov, S. G., Mazepa, V. S., Devi, N. M., Grigor'ev, A. A., Bartysch, A. A., Fomin, V. V., Kapralov, D. S., Terent'ev, M., Bugman, H., Rigling, A., and Moiseev, P. A., 2014: Treeline advance along the Ural mountain range—Driven by improved winter conditions? *Global Change Biology*, 20: 3530–3543.

Harsch, M. A., and Bader, M. Y., 2011: Treeline form—a potential key to understanding treeline dynamics. *Global Ecology and Biogeography*, 20: 582–596.

Hättenschwiler, S., and Smith, W. K., 1999: Seedling occurrence in alpine treeline conifers: a case study from the central Rocky Mountains, USA. *Acta Oecologica*, 20(3): 219–224.

Hessl, A. E., and Baker, W. L., 1997: Spruce and fir regeneration and climate in the forest-tundra ecotone of Rocky Mountain National Park, Colorado, U.S.A. *Arctic and Alpine Research*, 29(2): 173–183.

Hoch, G., and Körner, C., 2005: Growth, demography and carbon relations of *Polylepis* trees at the world's highest treeline. *Functional Ecology*, 19(6): 941–951.

Hoch, G., and Körner, C., 2009: Growth and carbon relations of tree line forming conifers at constant vs. variable low temperatures. *Journal of Ecology*, 97(1): 57–66.

Holtmeier, F. K., 2005: Relocation of snow and its effects in the treeline ecotone—with special regard to the Rocky Mountains, the Alps and Northern Europe. *Die Erde*, 136(4): 343–373.

Holtmeier, F. K., 2009: *Mountain Timberlines. Ecology, Patchiness, and Dynamics*. 2nd edition. New York: Springer, 438 pp.

Holtmeier, F. K., and Broll, G., 2005: Sensitivity and response of northern hemisphere altitudinal and polar treelines to environmental change at landscape and local scales. *Global Ecology and Biogeography*, 14(5): 395–410.

Holtmeier, F. K., and Broll, G., 2007: Treeline advance—driving processes and adverse factors. *Landscape Online*, 1: 1–32.

Holtmeier, F. K., and Broll, G., 2010: Altitudinal and polar treelines in the northern hemisphere—causes and response to climate change. *Polarforschung*, 79(3): 139–153.

IUSS Working Group WRB, 2006: *World Reference Base for Soil Resources 2006*. Rome: FAO, World Soil Resources Report No. 103, 133 pp.

Jacoby, G. C., and D'Arrigo, R. D., 1995: Tree-ring width and density evidence of climatic and potential forest change in Alaska. *Global Biogeochemical Cycles*, 9(2): 227–234.

Köhler, L., Gieger, T., and Leuschner, C., 2006: Altitudinal change in soil and foliar nutrient concentrations and in microclimate across the tree line on the subtropical island mountain Mt. Teide (Canary Islands). *Flora—Morphology, Distribution, Functional Ecology of Plants*, 201(3): 202–214.

Körner, C., 1998a: A re-assessement of high elevation treeline positions and their explanation. *Oecologia*, 115: 445–459.

Körner, C., 1998b: Worldwide position of alpine treelines and their causes. *In* Beniston, M., and Innes, J. L. (eds.), *The Impacts of Climate Variability on Forests*. Berlin-Heidelberg: Springer, pp. 221–229.

Körner, C., 2009: Mountain vegetation under environmental change. *Alpine Space – Man and Environment*, 7: 25–30.

Körner, C., 2012: *Alpine Treelines. Functional Ecology of the Global High Elevation Tree Limits*. Basel, Switzerland: Springer, 220 pp.

Körner, C., and Paulsen, J., 2004: A world-wide study of high altitude treeline temperatures. *Journal of Biogeography*, 31: 713–732.

Kullman, L., 2007: Tree line population monitoring of *Pinus sylvestris* in the Swedish Scandes, 1973–2005: implications for tree line theory and climate change ecology. *Journal of Ecology*, 95(1): 41–52.

Kupfer, J. A., and Cairns, D. M., 1996: The suitability of montane ecotones as indicators of global climatic change. *Progress in Physical Geography*, 20(3): 253–272.

Lara, A., Villalba, R., Wolodarsky-Franke, A., Aravena, J. C., Luckman, B. H., and Cuq, E., 2005: Spatial and temporal variation in *Nothofagus pumilio* growth at tree line along its latitudinal range (35°40′–55°S) in the Chilean Andes. *Journal of Biogeography*, 32: 879–893.

Larcher, W., 1957: Frosttrocknis an der Waldgrenze und in der alpinen Zwergstrauchheide. *Veröffentlichungen Museum Ferdinandeum Innsbruck*, 37: 49–81.

Larcher, W., 1963: Zur spätwinterlichen Erschwerung der Wasserbilanz von Holzpflanzen an der Waldgrenze. *Berichte des Naturwissenschaftlich-medizinischen Vereins in Innsbruck*, 53: 125–137.

Leuschner, C., 1996: Timberline and alpine vegetation on the tropical and warm-temperate oceanic islands of the world: elevation, structure and floristics. *Vegetatio*, 123: 193–206.

Leuschner, C., and Schulte, M., 1991: Microclimatic investigations in the tropical alpine scrub of Maui, Hawaii: evidence for a drought-induced alpine timberline. *Pacific Science*, 45: 152–168.

Liang, E., Dawadi, B., Pederson, N., and Eckstein, D., 2014: Is the growth of birch at the upper timberline in the Himalayas limited by moisture or by temperature? *Ecology*, 95(9): 2453–2465.

Liu, X., and Luo, T., 2011: Spatiotemporal variability of soil temperature and moisture across two contrasting timberline ecotones in the Sergyemla Mountains, Southeast Tibet. *Arctic, Antarctic, and Alpine Research*, 43(2): 229–238.

Lloyd, A. H., and Graumlich, L. J., 1997: Holocene dynamics of treeline forests in the Sierra Nevada. *Ecology*, 78(4): 1199–1210.

Loomis, P. F., Ruess, R. W., Sveinbjörnsson, B., and Kielland, K., 2006: Nitrogen cycling at treeline: latitudinal and elevational patterns across a boreal landscape. *Ecoscience*, 13(4): 544–556.

Macek, P., Klimeš, L., Adamec, L., Doležal, J., Chlumská, Z., and de Bello, F., 2012: Plant nutrient content does not simply increase with elevation under the extreme environmental conditions of Ladakh, NW Himalaya. *Arctic, Antarctic, and Alpine Research*, 44(1): 62–66.

Malanson, G. P., Resler, L. M., Bader, M. Y., Holtmeier, F. K., Butler, D. R., Weiss, D. J., Daniels, L. D., and Fagre, D. B., 2011: Mountain treelines: a roadmap for research orientation. *Arctic, Antarctic, and Alpine Research*, 43(2): 167–177.

Mayr, S., Hacke, U., Schmid, P., Schwienbacher, F., and Gruber, A., 2006: Frost drought in conifers at the alpine timberline: xylem dysfunction and adaptations. *Ecology*, 87(12): 3175–3185.

McNown, R. W., and Sullivan, P. F., 2013: Low photosynthesis of treeline white spruce is associated with limited soil nitrogen availability in the Western Brooks Range, Alaska. *Functional Ecology*, 27(3): 672–683.

Morales, M. S., Villalba, R., Grau, H. R., and Paolini, L., 2004: Rainfall-controlled tree growth in high-elevation subtropical treelines. *Ecology*, 85(11): 3080–3089.

Moyes, A. B., Germino, M. J., and Kueppers, L. M., 2015: Moisture rivals temperature in limiting photosynthesis by trees establishing beyond their cold-edge range limit under ambient and warmed conditions. *New Phytologist,* 207(4): 1005–1014.

Müller, M., Schickhoff, U., Scholten, T., Drollinger, S., Böhner, J., and Chaudhary, R. P., 2016: How do soil properties affect alpine treelines? General principles in a global perspective and novel findings from Rolwaling Himal, Nepal. *Progress in Physical Geography,* 40(1): 135–160.

Öberg, L., and Kullman, L., 2012: Contrasting short-term performance of mountain birch (*Betula pubescens* ssp. *czerepanovii*) treeline along a latitudinal continentality-maritimity gradient in the southern Swedish Scandes. *FENNIA*, 190(1): 19–40.

Oberhuber, W., 2004: Influence of climate on radial growth of *Pinus cembra* within the alpine timberline ecotone. *Tree Physiology*, 24: 291–301.

Oksanen, J., Blanchet, F. G., Kindt, R., Legendre, P., Minchin, P. R., O'Hara, B., Simpson,. G. L., Solymos, P., Stevens, M. H. H., and Wagner, H., 2015: vegan: Community Ecology Package. R package version 2.2-1. http://CRAN.R-project.org/package=vegan, accessed 6 January 2016.

Paulsen, J., and Körner, C., 2014: A climate-based model to predict potential treeline position around the globe. *Alpine Botany*, 124(1): 1–12.

Peters, T., Braeuning, A., Muenchow, J., and Richter, M., 2014: An ecological paradox: high species diversity and low position of the upper forest line in the Andean Depression. *Ecology and Evolution*, 4(11): 2134–2145.

Pohlert, T., 2014: Calculate pairwise multiple comparisons of mean rank sums (PMCMR). R package. http://www.project.org/web/packages/PMCMR/PMCMR.pdf, accessed 6 January 2016.

R Development Core Team, 2014: R: A language and environment for statistical computing. R Foundation for Statistical Computing, Vienna, Austria. http://www.R-project.org/, accessed 6 January 2016.

Richardson, A. D., and Friedland, A. J., 2009: A review of the theories to explain arctic and alpine treelines around the world. *Journal of Sustainable Forestry*, 28(1-2): 218–242.

Schickhoff, U., Bobrowski, M., Böhner, J., Bürzle, B., Chaudhary, R. P., Gerlitz, L., Heyken, H., Lange, J., Müller, M., Scholten, T., Schwab, N., and Wedegärtner, R., 2015: Do Himalayan treelines respond to recent climate change? An evaluation of sensitivity indicators. *Earth System Dynamics*, 6: 245–265.

Schwab, N., Schickhoff, U., Müller, M., Gerlitz, L., Bürzle, B., Böhner, J., Chaudhary, R. P., and Scholten, T., 2016: Treeline responsiveness to climate warming: insights from a krummholz treeline in Rolwaling Himal, Nepal. *In* Singh, R. B., Schickhoff, U., and Mal, S. (eds.), *Climate Change, Glacier Response, and Vegetation Dynamics in the Himalaya: Contributions Towards Future Earth Initiatives.* Basel, Switzerland: Springer, 307–346.

Shi, P., Körner, C., Hoch, G., 2008: A test of the growth-limitation theory for alpine tree line formation in evergreen and deciduous taxa of the eastern Himalayas. *Functional Ecology*, 22(2): 213–220.

Shrestha, B. B., 2007: Regeneration of treeline birch (*Betula utilis* D. Don) forest in a trans-himalayan dry valley in Central Nepal. *Mountain Research and Development*, 27(3): 259–267.

Slatyer, R. O., 1976: Water deficits in timberline trees in the Snowy Mountains of South-Eastern Australia. *Oecologia*, 24: 357–366.

Smith, W. K., Germino, M. J., Johnson, D. M., and Reinhardt, K., 2009: The altitude of alpine treeline: a bellwether of climate change effects. *Botanical Review*, 75: 163–190.

Soetaert, K., 2014: shape: Functions for plotting graphical shapes, colors. R package version 1.4.2. http://CRAN.R-project.org/package=shape, accessed 6 January 2016.

Stöhr, D., 2007: Soils—heterogeneous at a microscale. *In* Wieser, G., and Tausz, M. (eds.), *Trees at Their Upper Limit: Treelife Limitation at the Alpine Timberline*. Dordrecht: Springer.

Troll, C., 1961: Klima und Pflanzenkleid der Erde in dreidimensionaler Sicht. *Die Naturwissenschaften*, 48(9): 332–348.

Van Laar, A., and Akça, A., 2007: *Forest Mensuration*. Dordrecht: Springer, 385 pp.

Walter, H., and Medina, E., 1969: Die Bodentemperatur als ausschlaggebender Faktor für die Gliederung der alpinen und subalpinen Stufen in den Anden Venezuelas. *Berichte der Deutschen Botanischen Gesellschaft*, 82: 275–281.

Wardle, P., 1968: Engelmann Spruce (*Picea Engelmannii Engel.*) at its upper limits on the Front Range, Colorado. *Ecology Letters*, 49(3): 483–495.

Weisberg, P. J., and Baker, W. L., 1995: Spatial variation in tree regeneration in the forest-tundra ecotone, Rocky Mountain National Park, Colorado. *Canadian Journal of Forest Research*, 25(8): 1326–1339.

Wieser, G., and Tausz, M., 2007: *Trees at Their Upper Limit. Treelife Limitation at the Alpine Timberline*. Dordrecht: Springer, 232 pp.

Zeileis, A., and Grothendieck, G., 2005: zoo: S3 Infrastructure for Regular and Irregular Time Series. *Journal of Statistical Software*, 14(6): 1–27.

MS submitted 11 January 2016
MS accepted 1 June 2016